Journal of Sensor Science and Technology
Vol. 26, No. 4 (2017) pp. 235-238
http://dx.doi.org/10.5369/JSST.2017.26.4.235
pISSN 1225-5475/eISSN 2093-7563

Design and Vibration Analysis of Tri-axis Linear Vibratory MEMS Gyroscope

Seyeong Seok[1], Sanghee Moon[2], Kanghyun Kim[1], Suhyeon Kim[1], Seongjin Yang[1], and Geunbae Lim[1+]

Abstract

In this study, the design of a tri-axis micromachined gyroscope is proposed and the vibration characteristic of the structure is analyzed. Tri-axis vibratory gyroscopes that utilize Coriolis effect are the most commonly used micromachined inertial sensors because of their advantages, such as low cost, small packaging size, and low power consumption. The proposed design is a single structure with four proof masses, which are coupled to their adjacent ones. The coupling springs of the proof masses orthogonally transfer the driving vibrational motion. The resonant frequencies of the gyroscope are analyzed by finite element method (FEM) simulation. The suspension beam spring design of proof masses limits the resonance frequencies of four modes, viz., drive mode, pitch, roll and yaw sensing mode in the range of 110 Hz near 21 kHz, 21173 Hz, 21239 Hz, 21244 Hz, and 21280 Hz, respectively. The unwanted modes are separated from the drive and sense modes by more than 700 Hz. Thereafter the drive and the sense mode vibrations are calculated and simulated to confirm the driving feasibility and estimate the sensitivity of the gyroscope. The cross-axis sensitivities caused by driving motion are 1.5 deg/s for both x- and y-axis, and 0.2 deg/s for z-axis.

Keywords: MEMS, Gyroscope, FEM Simulation

1. INTRODUCTION

A gyroscope is an instrument that is used to measure the angular velocity of an object. Micromachined gyroscopes have been drawing interest of commercial industries with the development of Microelectromechanical system (MEMS) technologies due to their advantages e.g., low cost, small size and mass producible fabrication throughput [1-3]. Most micromachined gyroscopes are based on vibratory structure utilizing Coriolis Effect that transfers energy between two orthogonal vibrational modes, drive mode and sense mode. Single-axis, especially z-axis micromachined gyroscopes had been the most researched type until a few years ago.

Recently, tri-axis gyroscopes have been drawing interests of researchers because of their advantages over multiple single-axis gyroscopes, such as circuitry simplicity, system configuration, and low power consumption [4,5].

The important structural requirements of a tri-axis gyroscope are four degrees of freedom (DoF), i.e., one drive mode and three sense modes, and decoupling of the four modes. Usually, the drive mode is similar to that of tuning fork gyroscopes – sets of proof masses facing each other, vibrate against each other symmetrically.

Another requirement is that there must be at least two orthogonal drive mode vibrations, because Coriolis force does not exist when the external angular velocity is parallel with the drive mode. Since the quality factor of in-plane vibration for silicon structure is much higher than that of out-of-plane vibration and the fabrication process of comb drive structure is simple, almost all tri-axis gyroscopes adopt x- and y-axis in-plane drive direction by capacitive comb structures.

Tri-axis vibratory gyroscope structures reported to date are mostly linear vibratory gyroscopes [5-8], while vibrating wheel gyroscopes[9,10] have also been studied by a few groups.

Tri-axis linear vibratory gyroscope uses drive mode like a tuning fork. As they need two driving directions, two orthogonally placed sets of proof masses facing each other are needed and anchor placed between them causes anchor loss while driving.

Vibrating wheel gyroscope has monolithic-wheel shaped single proof mass, and the drive mode is z-axis in-plane rotation of the wheel. The rotational movement demands circular beam springs

[1]Department of Mechanical Engineering, Pohang Univer sity of Science and Technology, 77 Cheongam-ro, Nam-gu, Pohang, Gyeongsangbuk-do, 37673, Rep. of Korea.
[2]Standing Egg Inc., Twosun World Building 7F, 221 Pangyoyeok-ro, Bundang-gu, Seongnam-si, Gyeonggi-do, 13494, Korea
[+]Corresponding author: limmems@postech.ac.kr
(Received: Jul. 19, 2017, Accepted: Jul. 27, 2017)

and capacitive sensing structures that leads to complicated design fabrication processes.

Here, we present a single-structure tri-axis linear vibratory gyroscope with vibrating-wheel-like drive mode. Four masses are coupled by anchorless coupling springs and are driven by capacitive comb drive electrodes, decoupled to limit the driving motion in only the desired direction. Two sense modes are out-of-plane and one is along the in-plane direction.

2. METHOD

2.1 Operation Principle

The operation principle of vibratory gyroscope is shown in Fig. 1. The proof mass resonates along the drive direction. When an external angular velocity is applied, Coriolis force orthogonal to both drive direction and external rotation acts on the proof mass, resulting in sense mode vibration. The frequency of sense mode vibration is the same as that of the drive mode, because the Coriolis force acting on the proof mass is proportional to velocity of the mass, *v*, which is a result of driving.

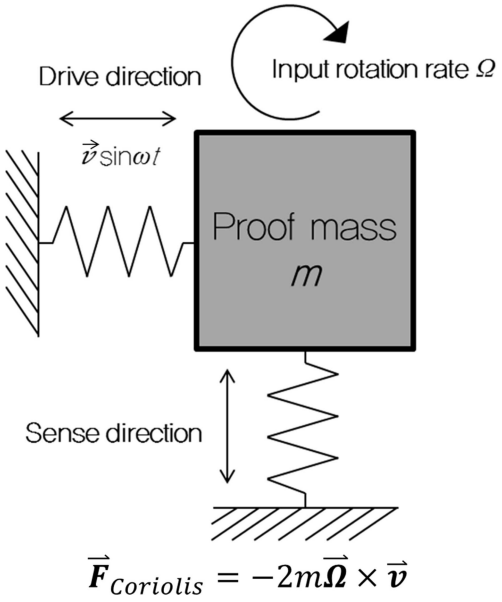

Fig. 1. Operation principle of Coriolis vibratory gyroscope

2.2 Structural design

The overall structure size is 1600 μm x 1600 μm with the thickness of 25 μm. As tri-axis gyroscopes require two drive directions, four proof masses are used as shown in Fig. 2. When x-axis angular velocity is applied, Coriolis force in the direction of

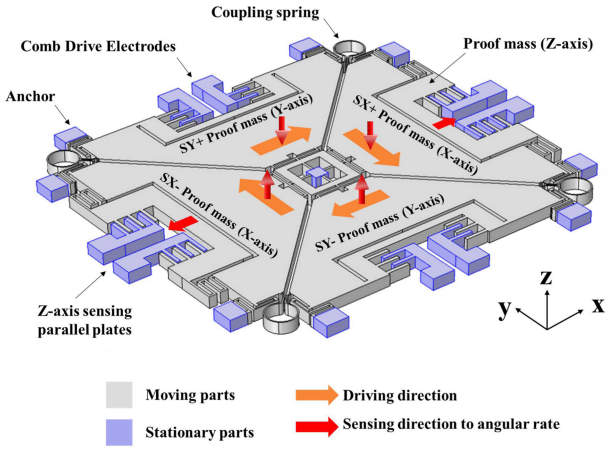

Fig. 2. Schematic diagram showing the structure and operation principle of the gyroscope

out-of-plane z-axis acts on proof masses SX+ and SX-, and their sense mode oscillation is sensed differentially by capacitive electrodes placed at a distance of 3 μm under the structure. Similarly, y-axis angular velocity is sensed by electrodes under SY+ and SY-. When z-axis angular velocity is applied, the Z-sensing differential parallel plates are forced to vibrate along the x-axis, or centrifugal direction. The differential sensing is applied to minimize the effect of acceleration

The driving force is only applied to two proof masses, and orthogonal transfer of the driving motion is coupled by coupling spring positioned between the proof masses. The proof masses are anchored to L-shaped anchor springs, allowing only the drive mode and out-of-plane sensing mode.

3. RESULTS AND DISCUSSIONS

The simulation is conducted with COMSOL Multiphysics. The mesh is generated by swept method with 3 layers, with the maximum and minimum element size, and element growth rate being 47 μm, 2 μm, and 1.35, respectively.

3.1 Resonant frequency

The resonant frequencies are designed to be around 20 kHz to avoid interference with external noises. The frequency split between the modes is necessary to avoid unwanted vibrational coupling, but the amount of the split should be small to attain high sensitivity. As shown in Fig. 3, the resonant frequencies are located around 21.1 kHz, and the difference between the lowest and the highest resonant frequency is about 0.5%.

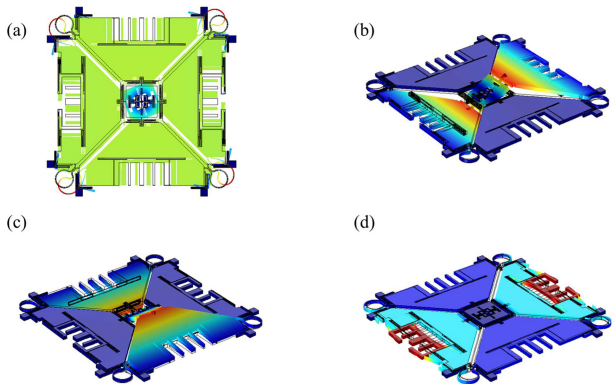

Fig. 3. The resonance frequency shapes of drive and sense modes. (a) drive mode at 21,173 Hz, (b) X-sense mode at 21,239 Hz, (c) Y-sense mode at 21,244 Hz, (d) Z-sense mode at 21,280 Hz.

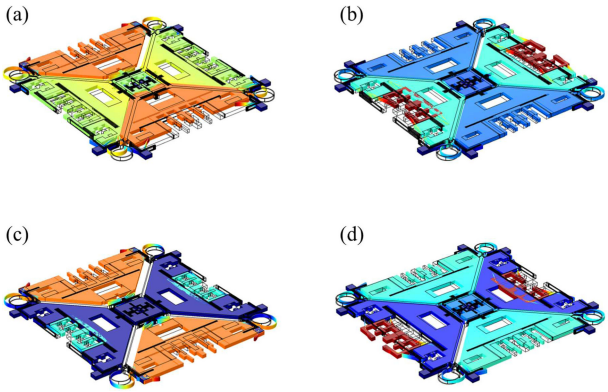

Fig. 4. Unwanted resonance frequencies. (a) 19,114 Hz, (b) 19,349 Hz, (c) 26,020 Hz, (d) 26,882 Hz

Separation of the resonance frequencies of the unwanted modes is also an important part of gyroscope design. In this design, unwanted modes have been separated by more than 0.7 kHz from the drive and sense modes, as shown in Fig. 4.

3.2 Drive mode analysis

The driving is initiated by comb drive electrodes located at SX+ and SX- proof masses. The linear vibration is coupled to SY+ and SY- proof masses via coupling springs. The importance of transferring vibration to orthogonal direction is critical for the proposed gyroscope. Fig. 5 shows that the simulated displacement difference between proof masses in drive mode is only 1.967%. The SX and SY proof mass values in the figure represent the displacements of the proof masses in x-, and y- direction, respectively.

The maximum displacement of drive mode with driving voltage of 3V peak-to-peak is simulated to be 3.94 μm (estimated quality

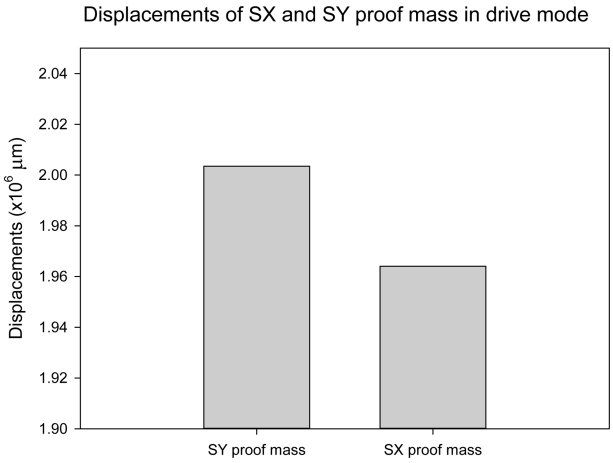

Fig. 5. Displacements of proof mass in drive mode resonance frequency analysis

factor ~ 5,000). The Coriolis force for maximum displacement can be calculated by obtaining velocity from resonant frequency and displacement.

Let *X, A,* ωbe the displacement of the mass at time *t*, maximum displacement, and drive mode frequency, respectively, then

$$X = A \sin \omega t = 3.94 \times 10^{-6} \sin(21173 \times 2\pi t) \quad (1)$$

Differentiating with respect to t yields

$$v = \frac{dX}{dt} = A\omega \cos\omega t$$

$$= 3.94 \cdot 10^{-6} \cdot 21173 \cdot 2\pi \cos(21173 \cdot 2\pi t) = 0.524 m/s \quad (2)$$

The maximum Coriolis force $F_{Coriolis} = 2mv \times \Omega$. When an external angular velocity of 1 deg/s is applied, the Coriolis force for x-, y-and z-axis sense modes are 1.27×10^{-8} N, 1.244×10^{-8} N and , 1.77×10^{-9} N where $m_{SX} = 1.21 \times 10^{-8}$ kg, $m_{SY} = 1.21 \times 10^{-8}$ kg and $m_{SZ} = 1.69 \times 10^{-9}$ kg, respectively.

3.3 Sense mode analysis

Coriolis force calculated before can be used to calculate the estimated sensitivity of the gyroscope. The average simulated displacement under Coriolis force with angular velocity of 1 deg/s is 5.1nm, 5.1 nm and 93 nm for x-, y-, and z-axis respectively.

Usually, the minimum amount of capacitance change a charge amplifier can measure is known to be around 2 fF. Converting the displacement into capacitance change yields the minimum detectable angular velocity to be 1.5 deg/s for both x- and y-axis, 0.2 deg/s for z-axis.

Table 1. Cross-axis displacement simulation result and equivalent rate of sense modes caused by driving motion.

Axis	Expression	Value	Equivalent angular velocity
x-axis	$\frac{\text{disp. SY in z axis}}{\text{disp. SY in x axis}}$	1.31×10^{-6}	2.5×10^{-4} deg/s
y-axis	$\frac{\text{disp. SX in z axis}}{\text{disp. SX in y axis}}$	2.98×10^{-6}	5.4×10^{-4} deg/s
z-axis	$\frac{\text{disp. SX in x axis}}{\text{disp. SX in y axis}}$	1.2×10^{-3}	0.013 deg/s

The sense mode displacements and capacitive outputs are affected by drive mode cross-axis sensitivity, since the sense mode displacement is relatively small compared to driving magnitude. Cross-axis displacement is defined as unwanted sense mode displacement divided by desired driving displacement, and the simulated results are presented in Table 1. The cross-axis values are close to one in a million for out-of-plane sense modes, and 0.0012 for z-axis sense mode, which is equivalent to angular velocity of 0.00025 deg/s, 0.00054 deg/s, and 0.013 deg/s for x-, y-, and z-axis respectively.

4. CONCLUSIONS

In this study, a linear vibratory tri-axis gyroscope that combines a linear vibratory structure with vibrating wheel motion is designed and its vibration characteristics are simulated. The drive mode and x-, y- and z-axis sense mode resonance frequencies are found to be 21,173 Hz, 21,2 39 Hz, 21,244 Hz and 21,280 Hz, respectively. Unwanted resonance modes are separated by 700 Hz. Coriolis force is then calculated from the drive mode displacement. Sensitivity limit of the gyroscope is also investigated using the simulated values to determine the performance limit. The cross-axis sensitivity shows that the structure is robust to cross-axis error due to driving motion.

ACKNOWLEDGMENT

This research was supported by Standing Egg Inc and the work was supported by the National Research Foundation of Korea (NRF) grant funded by the Korea government (MSIP) (NO. 2015R1A2A1A14027903).

REFERENCES

[1] N. Yazdi, F. Ayazi, and K. Najafi, "Micromachined inertial sensors," *Proc. IEEE*, Vol. 86, No. 8, pp. 1640-1659, Aug. 1998.

[2] K. Liu *et al.*, "The development of micro-gyroscope technology," *J. Micromech. Microeng.*, Vol. 19, No. 11, p. 113001, 2009.

[3] D. Xia, C. Yu, and L. Kong, "The development of micromachined gyroscope structure and circuitry technology," *Sensors*, Vol. 14, No. 1, pp. 1394-1473, Jan. 2014.

[4] J. Sung *et al.*, "A gyroscope fabrication method for high sensitivity and robustness to fabrication tolerances," *J. Micromech. Microeng.*, Vol. 24, No. 7, p. 075013, 2014.

[5] D. Xia, L. Kong, and H. Gao, "Design and analysis of a novel fully decoupled tri-axis linear vibratory gyroscope with matched modes," *Sensors*, Vol. 15, No. 7, pp. 16929-16955, Jul. 2015.

[6] S. Sonmezoglu *et al.*, "Single-Structure Micromachined Three-Axis Gyroscope with Reduced Drive-Force Coupling," *IEEE Electron Device Lett.*, Vol. 36, No. 9, pp. 953-956, Sep. 2015.

[7] S. Wisher *et al.*, "A high-frequency epitaxially encapsulated single-drive quad-mass tri-axial resonant tuning fork gyroscope," in *2016 IEEE 29th Int. Conf. on Micro Electro Mech. Syst. (MEMS)*, 2016, pp. 930-933.

[8] M. A. Shah, F. Iqbal, I. A. Shah, and B. Lee, "Modal Analysis of a Single-Structure Multiaxis MEMS Gyroscope," *J. Sensors*, 2016. [Online]. Available: https://www.hindawi.com/journals/js/2016/4615389/. [Accessed: 06-Jul-2017].

[9] N. C. Tsai and C. Y. Sue, "Design and Analysis of a Tri-Axis Gyroscope Micromachined by Surface Fabrication," *IEEE Sensors. J.*, vol. 8, no. 12, pp. 1933–1940, Dec. 2008.

[10] D. Xia, L. Kong, and H. Gao, "A Mode Matched Triaxial Vibratory Wheel Gyroscope with Fully Decoupled Structure," *Sensors*, Vol. 15, No. 11, pp. 28979-29002, Nov. 2015.